

# **Blind Source-Separation for Heart Wall and Erythrocyte Motion Estimation in the Beating Embryonic Heart**

**Sandeep Bhat**  
Systems Bioimaging Lab, UCSB  
sandeepkbhat@ece.ucsb.edu

November 13, 2008

## **Abstract**

Bright-field microscopy can be used for high speed imaging of unstained biological samples. However, the images lack the specificity seen in fluorescence microscopy. The paper discusses an algorithm that helps improve the specificity of structures present in bright-field microscopy images, particularly with respect to the imaging of the beating embryonic zebrafish heart. The algorithm, separates the bright-field microscopy image sequence of the beating embryonic heart into two image sequences. One sequence shows only the heart morphology, without any structures that float in the blood (e.g. red blood cells) and the other shows only these transient structures. The two image sequences can then be analyzed separately to characterize the motion of the blood cells and the heart wall.

# Contents

<b>1</b>	<b>Introduction</b>	<b>4</b>
<b>2</b>	<b>The Separation Algorithm</b>	<b>6</b>
2.1	Pre-processing Stage . . . . .	7
2.1.1	Manual estimation of period . . . . .	7
2.1.2	Rearrangement and temporal alignment . . . . .	7
2.2	HW-RBC Algorithm . . . . .	9
2.2.1	Separation of heart-wall images . . . . .	9
2.2.2	Separation of RBC images . . . . .	11
2.3	Post-processing stage . . . . .	12
<b>3</b>	<b>Implementation and Testing</b>	<b>13</b>
3.1	Algorithm inputs . . . . .	13
3.2	Algorithm outputs . . . . .	13
3.3	Algorithm assessment using synthetic heartbeat data . . . . .	14
3.3.1	Heart-wall Data Generation . . . . .	14
3.3.2	RBC Data Generation . . . . .	15
3.3.3	Heartbeat Data Composition . . . . .	15
<b>4</b>	<b>Results and Observations</b>	<b>17</b>
<b>5</b>	<b>Conclusion</b>	<b>22</b>
	<b>Acknowledgements</b>	<b>22</b>
	<b>Bibliography</b>	<b>23</b>

# List of Figures

2.1	Top-level block diagram . . . . .	8
2.2	Pixel-intensity variation with time . . . . .	9
2.3	Heart-wall extraction steps . . . . .	10
4.1	Mean filtering on high frame-rate heart data . . . . .	17
4.2	Median filtering on high frame-rate heart data . . . . .	17
4.3	Mean filtering on medium frame-rate heart data . . . . .	18
4.4	Median filtering on medium frame-rate heart data . . . . .	18
4.5	Mean filtering on synthetic heart data . . . . .	19
4.6	Median filtering on synthetic heart data . . . . .	19
4.7	Mean filtering on synthetic heart data . . . . .	20
4.8	Median filtering on synthetic heart data . . . . .	20
4.9	Flow analysis on the separated image sequences . . . . .	21

# List of Tables

4.1	Separation results for high frame-rate heart data . . . . .	18
4.2	Separation results for medium frame-rate heart data . . . . .	19
4.3	Separation results for synthetic heart data . . . . .	20

# Chapter 1

## Introduction

The study of biological phenomena in model organisms provides insights into the workings of other organisms. In particular, model organisms are widely used to understand the potential causes and treatments for human disease when experiments on humans would not be feasible or ethical. Zebrafish (*Danio rerio*) has a nearly transparent body during early development, which provides unique visual access to the animal's internal anatomy. Therefore, it is used as a model organism to study embryonic development, toxicology and specific gene function. The aim of this work is to develop an algorithm that would aid the live imaging of the developing zebrafish heart.

Live imaging of the zebrafish heart is helpful in quantifying force relationships and studying morphogenetic movements in the developing embryos. The heart-wall motions and blood flow in the embryonic heart are fast (several millimeters per second) and need high frame-rates to be imaged without motion artifacts like aliasing and blurring [1]. Therefore, live imaging requires dynamic methods that offer high spatial and temporal resolution. Two widely used methods are fluorescence microscopy and bright-field microscopy.

In fluorescence microscopy, the different structures of the specimen are labeled with different chemicals (fluorophores) that when illuminated with light of specific wavelength exhibit fluorescence. Multi-color images of the specimen can be created by putting together the different fluorescence images, thereby providing a high degree of specificity [2]. However, the cost and complexity of the equipment and sample preparation are high. Also, the frame rates possible with current techniques of fluorescence microscopy are not sufficient for effective flow analysis.

In contrast, bright-field microscopy requires a basic setup and no sample

preparation. It also achieves high imaging speeds, thereby enabling easy imaging of live cells. However, it suffers from poor contrast and has low apparent optical resolution due to blurring of the out-of-focus material [3, 4]. These issues result in the lack of specificity in imaging unstained biological samples.

For the flow analysis to be effective on bright-field microscopy images, novel image processing techniques are required to “separate” the structures present. Here “separation” refers to the segmentation of the heart images into different regions: one with the heart wall and the other with red blood cells (RBCs). General image segmentation techniques [5] can be applied on each image in the sequence. Though this would produce the desired output, it does not take advantage of the periodicity of the beating heart-wall or the similarity between images taken at equivalent time points in the cardiac cycle [6].

The algorithm developed in this work takes these factors into account and separates the bright-field microscopy image sequence of the beating embryonic heart into two image sequences. One sequence shows only the heart morphology without the RBCs, while the other sequence shows only the transient structures of the blood, mainly the RBCs. The two sequences can then be analyzed to characterize motion of the blood and heart-wall separately.

This report is organized as follows. Section 1 gives the context and the motivation for this project. Section 2 discusses the separation algorithm in detail. Section 3 provides the implementation and testing details. Section 4 presents the results and observations. Section 5 summarizes the algorithm and presents the scope for future work.

## Chapter 2

# The Separation Algorithm

This chapter discusses the heart wall and RBC separation algorithm in detail. The input image sequence comprises of several periods of the beating heart. These images exhibit the flow of RBCs, the beating heart wall and the static background. The motion of the beating heart wall is mostly “periodic.” On the contrary, the flow of RBCs in the blood is non-periodic. This fact can be used to separate the two from the bright-field microscopy image sequence.

Assuming the inter-frame interval remains constant for the entire duration of the sequence capture, the period of heart beat can be taken to be  $T$  frames. If the total sequence is comprised of  $N$  whole periods, the  $2D+time$  image sequence (with  $N \times T$  frames) could be rearranged into  $N$  sequences each containing  $T$  frames. Since the heart wall is periodic, the  $i$ th frame of all  $N$  sequences correspond to a similar position of the heart wall in the cardiac cycle. This could be used to separate the heart wall and the static background from the images.

However the assumption that the total period is an integer number of frames does not always hold. Also temporal inter-frame variations and slight irregularities in the heart beat could produce severe visual artifacts in the separated sequences thereby rendering them useless for further analysis. Therefore temporal synchronization needs to be done on the sequence before separating the heart-wall.

A technique for 3D dynamic data reconstruction after temporal alignment of nongated slice-sequences acquired at different axial positions in the heart of a zebrafish embryo was proposed in [1]. The  $2D+time$  data can be rearranged into  $3D+time$  using an estimate of the time period as described in [6]. This  $3D+time$  data would comprise of multiple image sequences, each spanning at least one period of the heart beat. The rearranged data

can then be temporally aligned as suggested in [1] before separating the heart-wall and the RBC.

The algorithm developed in this work can be split into three stages: the pre-processing stage, the main algorithm and the post-processing or the analysis stage. The pre-processing stage is based entirely on the techniques developed in [1, 6]. The main algorithm, referred from this point on as HW-RBC algorithm, is based on the fact that the heart wall motion is “periodic” while the RBC flow is not. The optional post-processing stage involves analysis of the heart-wall and RBC sequences to extract flow maps. Figure 2.1 shows the top-level block diagram illustrating the various stages of the algorithm. These are discussed in greater detail in the following sections.

## 2.1 Pre-processing Stage

The pre-processing stage of the algorithm consists of two main steps. The first is the estimation of the heart period. The second step involves rearranging the input  $2D+time$  image sequence into a temporally aligned  $3D+time$  sequence based on the period estimate from the previous step. This step takes care of visual artifacts that might occur in the separated heart-wall and RBC sequences due to a wrong period estimate.

### 2.1.1 Manual estimation of period

In the input  $2D+time$  image sequence of the beating heart, the variation of pixel intensity at a particular point with time is more or less periodic. The red region in Figure 2.2.a shows typical variations in pixel-intensity with time over the entire sequence. The red region in Figure 2.2.b shows the variation over the manually chosen frames that approximately span 3 cardiac cycles. The green regions are repeated version of the red regions. This is to ensure continuity across periods and validate the estimated period. By considering the intensity variations at several locations in the image, an average estimate for the heart beat period can be found. For better estimates, the locations can be manually confined to be in the region of the heart-wall, the truly “periodic” part of the heart.

### 2.1.2 Rearrangement and temporal alignment

In the next step, the  $2D+time$  image sequence is rearranged into  $3D+time$  sequence based on the estimated period. In order to effectively separate the “periodic” heart-wall we first need to temporally align the frames in the  $3D+time$  sequence so that there is maximum similarity between the frames that have been captured at equivalent time points in the cardiac cycle.

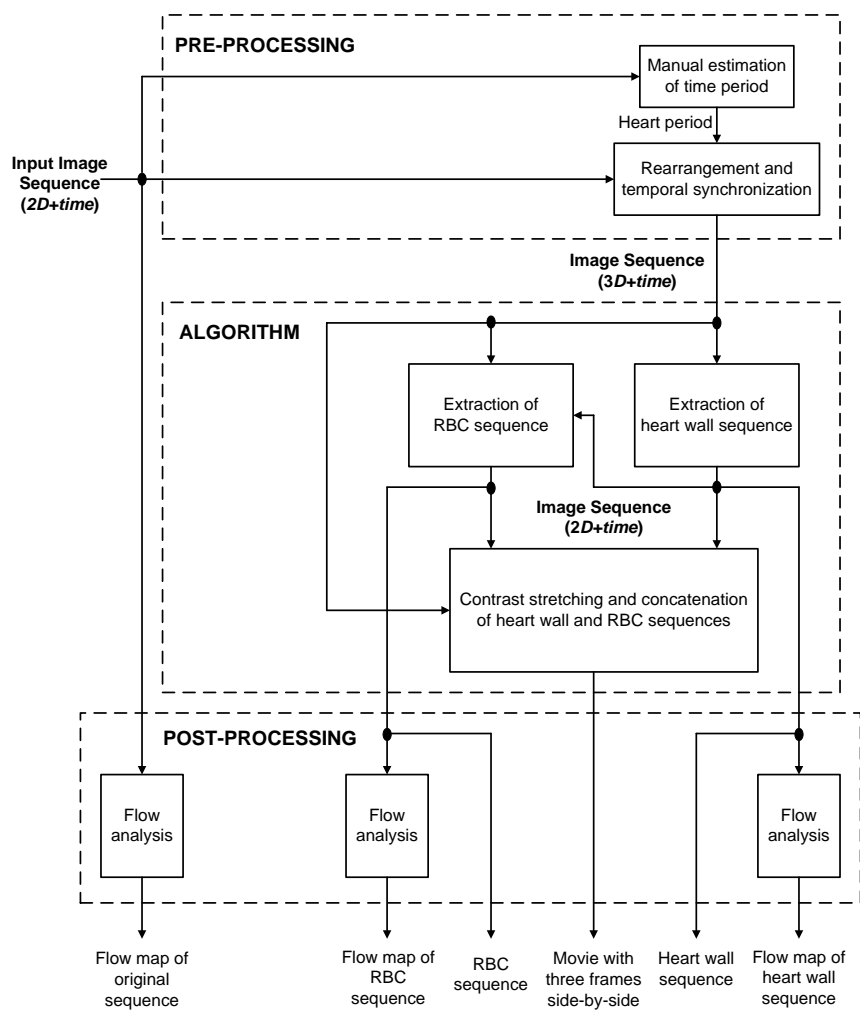


**Figure 2.1:** Top-level block diagram. The dotted boxes indicate the various stages of the algorithm.

The Z-dimension in the 3D data corresponds to the sequence number or the “repeat.” The frames belonging to different repeats can be temporally aligned using a nonuniform time-registration method suggested in [1, 7].

This technique crops each of the repeat-sequence to span an integer number of periods and interpolates them in time so that sequences have the same number of frames. Each sequence is then shifted in time such that the frames in the different repeats are synchronized. The amount of shift is decided based on the minimization of the absolute value of the intensity difference between adjacent repeat sequence pairs. These steps are summarized in Figure 2.3.

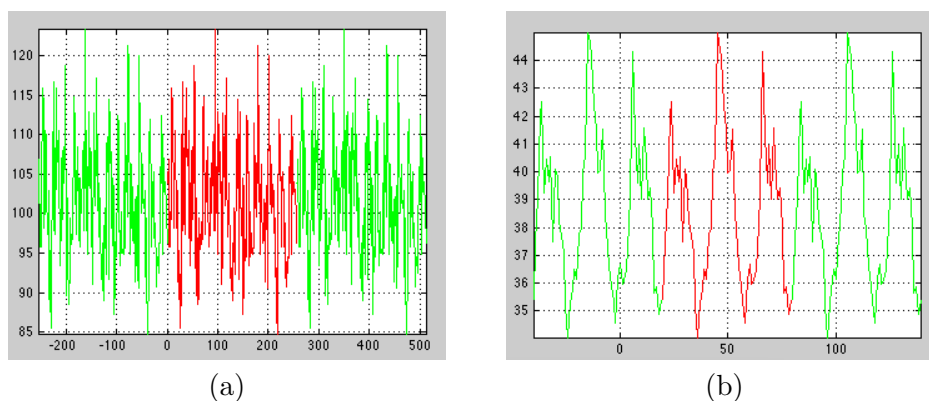


**Figure 2.2:** Pixel-intensity variation with time at a particular location for a bright-field microscopy image sequence of the beating embryonic heart. (a) The red region shows the variation over the whole sequence of 256 frames (b)The red region shows the variation for 3 cardiac cycles. The green regions to the left and right repeat the same variation to help validate the estimated period

## 2.2 HW-RBC Algorithm

The algorithm used for the separation of the heart-wall and RBC images is called the HW-RBC algorithm. This section first discusses the techniques used for the extraction of the heart-wall images. Finally methods to separate the RBC images are discussed.

### 2.2.1 Separation of heart-wall images

In the temporal aligned  $3D+time$  sequence, the heart-wall is mostly static in the frames along the repeat direction. Two techniques that separate the heart-wall based on this are described below.

Let  $I(x, y, z, t)$  be the  $3D+time$  data with  $0 \leq x < W$ ,  $0 \leq y < H$ ,  $0 \leq z < N$  and  $0 \leq t < T$ . Here  $W$  is the frame width,  $H$  is the frame height,  $N$  is the number of repeats and  $T$  is the number of frames in each of the repeats. Then the heart-wall sequence can be got as the mean of  $I(x, y, z, t)$  along the repeat ( $z$ ) direction.

$$I_{HW}(x, y, t) = \frac{1}{N} \sum_{z=0}^{N-1} I(x, y, z, t) \quad (2.1)$$

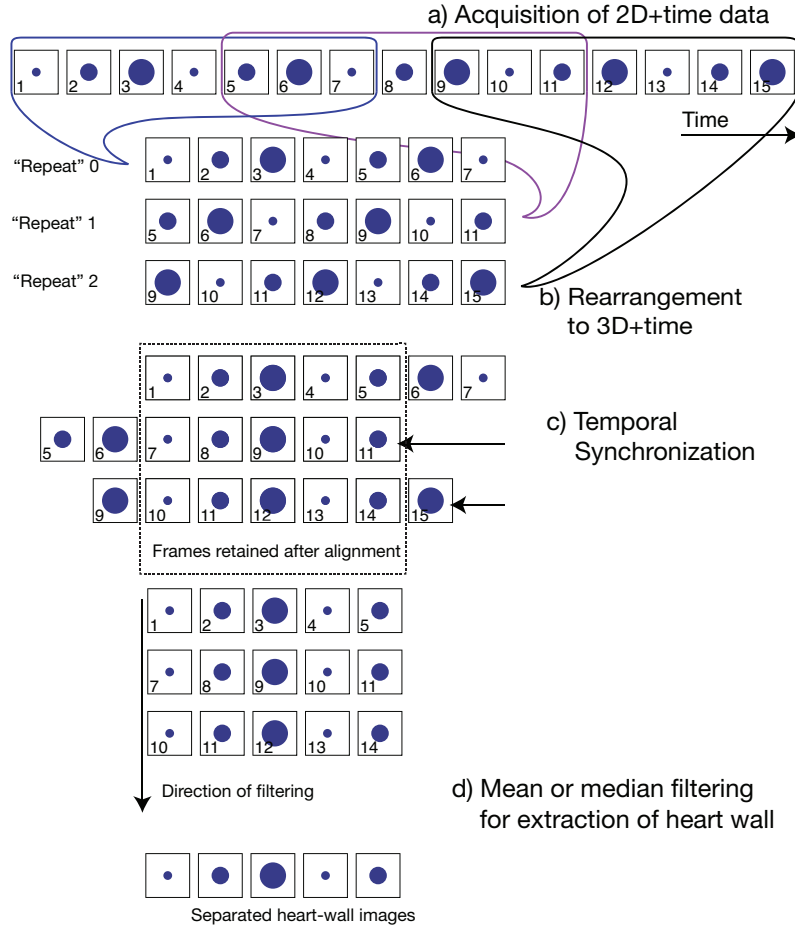


**Figure 2.3:** Frame diagram illustrating the various steps involved in the extraction of heart-wall. a) Frames of the input sequence. The frame numbers are indicated at the bottom left of each frame. b) Rearrangement of the frames according to the estimated period. Note that some frames from “Repeat” 0 are replicated in “Repeat” 1 to ensure good synchronization [6]. c) Temporal alignment through shifting of the repeat-sequences in time [1]. d) Mean or median filtering along the repeat direction to extract the heart-wall sequence.

The heart-wall sequence could also be obtained as the median of  $I(x, y, z, t)$  along the repeat ( $z$ ) direction. Let  $I_{(0)}(x, y, t), I_{(1)}(x, y, t), \dots, I_{(N-1)}(x, y, t)$  be the order statistics of the data along the  $z$ -direction with  $I_{(0)}(x, y, t) \leq I_{(1)}(x, y, t) \leq \dots \leq I_{(N-1)}(x, y, t)$ . Then the median along the  $z$ -direction is defined as [8]

$$I_{HW}(x, y, t) = \begin{cases} I_{(N-1)}(x, y, t) & , \text{ when } N \text{ is odd} \\ \frac{1}{2}(I_{(\frac{N}{2}-1)}(x, y, t) + I_{(\frac{N}{2})}(x, y, t)) & , \text{ when } N \text{ is even} \end{cases} \quad (2.2)$$

Thus the pixels belonging to the heart-wall can be separated by simple mean or median filtering along the repeat direction. Note that the resulting heart-wall sequence is only  $2D+time$ . Also the static background present in the original image sequence is retained in the resulting heart-wall sequence.

This heart-wall separation technique can be perceived as a form of “denoising”. In the the frames along the repeat direction, the pixels belonging to RBCs are never at the same location unlike the pixels that belong to the heart-wall. So the RBC pixels can be treated as “noise” and can be removed using an averaging filter (mean) or an order statistics filter (median) [9]. Once the pixels belonging to the RBCs are “averaged” out the “static” regions belonging to the heart-wall are left behind in the images.

### 2.2.2 Separation of RBC images

The RBC images can be got by removing the separated heart-wall from the original sequence. The separated heart-wall data is  $2D+time$  whereas the original data input to this stage is  $3D+time$ . There are two ways in which this can be handled.

The first method is simple subtraction. In this technique one of the sequences present in the aligned  $3D+time$  data is chosen as the reference sequence. The extracted heart-wall is then subtracted from this sequence to get the RBCs. This is summarized in the equation below. Let  $I_{HW}(x, y, t)$  be the heart-wall sequence got using either equation 2.1 or 2.2. Let  $I_{REF}(x, y, t) = I(x, y, z_{REF}, t)$  be the reference sequence. Then the RBC sequence is given by

$$I_{RBC}(x, y, t) = I_{REF}(x, y, t) - I_{HW}(x, y, t) \quad (2.3)$$

The second method is the variance method. In this technique the RBC images are extracted as the “variance” of the aligned  $3D+time$  data along the repeat direction.

$$I_{RBC}(x, y, t) = \frac{1}{N} \sum_{z=0}^{N-1} |I(x, y, z, t) - I_{HW}(x, y, t)|^2 \quad (2.4)$$

$I_{HW}(x, y, t)$  is the heart-wall sequence got by using either equation 2.1 or 2.2.

As suggested towards the end of section 2.2.1, the RBC images manifest themselves as high-frequency noise. So they can be “filtered” out in the frequency domain. First the 1-D Discrete Fourier Transform (DFT) is applied on the aligned  $3D+time$  sequence along the repeat dimension. Then using a high pass filter, the high frequency components corresponding to the flowing RBCs are retained. The filtered output is then inverse transformed to get the RBC images. Unlike the subtraction or the variance method, this technique does not depend on the heart-wall sequence extracted previously.

### 2.3 Post-processing stage

The optional post-processing stage involves the analysis of the separated heart-wall and RBC sequences in image visualization softwares like ImageJ or Imaris. In particular, the FlowJ plugin of ImageJ [10] can be used for flow analysis on the sequences to extract the flow map.

## Chapter 3

# Implementation and Testing

This chapter discusses the implementation details of the algorithm and its testing. The pre-processing and the HW-RBC algorithm were implemented in MATLAB. The post-processing stage was accomplished using FlowJ plugin in ImageJ. The parameters for the flow analysis were set according to [10]. The results and the observations are included at the end of the chapter.

### 3.1 Algorithm inputs

The input image sequence comprises of several periods of the beating embryonic heart. This time series data is acquired sequentially at a fixed focal plane using a bright-field microscope. No external gating signals are used during the acquisition of the images. These images are then saved as 5-dimensional OME-XML files [11].

### 3.2 Algorithm outputs

The output from the algorithm comprises of two image sequences spanning at least one period of the beating heart. The algorithm generates these images in OME format. The extracted  $2D+time$  heart-wall and RBC sequences are converted to 5D data by addition of two dummy singleton dimensions before being saved into OME files. The addition of dummy dimensions does not effect the images in any way.

The image data is processed by the HW-RBC algorithm and saved into OME files as *single* datatype. This provides a wide dynamic range ( $\approx 6.8 \times 10^{38}$ ) for image representation. For ease of visualization, frames from the reference (original data), the heart-wall and the RBC sequences are subjected to dynamic contrast stretching and concatenated side-by-side

to create a composite frame sequence. Figure 4.1 shows a composite frame.

The separated heart-wall and RBC images can also be analyzed separately for systematic characterization of the developing heart in a zebrafish embryo. In particular flow analysis is done using FlowJ on the original sequence and the separated heart-wall and RBC sequences. The flow-map sequences are obtained as dynamic color(DC) maps where the type of color indicates the orientation and the intensity of the color indicates the velocity of flow [10]. These flow-map sequences are shorter in length (total number of frames) than the original sequence due to the minimum support frames needed for flow analysis. The flow-map sequences from the original sequence, the heart-wall and the RBC sequences are concatenated side-by-side to create a composite flow-map sequence. Figure 4.9 shows a composite flow-map frame.

### 3.3 Algorithm assessment using synthetic heartbeat data

Synthetic heartbeat data generation is the process of generating an image sequence that models the working of a beating embryonic zebrafish heart, particularly the periodic motion of the heart-wall (HW) and the random motion of the red blood cells (RBC). The data generated is used to test the effectiveness of HW-RBC algorithms that separate the heart-wall and the RBC images from composite images of the beating heart.

The heart-wall and RBC images separated using the HW-RBC algorithm can be visually compared with the original image sequence to verify the quality of separation. A better approach would be to compare the two image sequences obtained against the ground-truth generated using fluorescence microscopy. However, this data is not easy to generate and therefore other methods need to be adopted to assess the quality of separation.

Instead of using actual heart data to test the algorithms, synthetic test data that mimics the beating of the heart can be used. The process discussed here generates such synthetic data and involves the following stages: heart-wall data generation, RBC data generation, and heart-beat data composition.

#### 3.3.1 Heart-wall Data Generation

This stage generates the periodic “heart-wall” image sequence as follows:

- A textured grayscale image that looks like the heart-wall of zebrafish embryo is first chosen. Usually, a close-up image of a leaf showing the veins works well.
- The period  $T$  of the heart-wall and the number of periods  $N$  is chosen. The final heart-wall sequence would have  $N \times T$  frames.
- The starting frame is then selected by choosing an origin  $(x, y)$  and a bounding box of size  $W \times H$  pixels in the textured grayscale image. The pixels in this selection are then cropped to make up a frame of the heart-wall sequence.
- The subsequent frames of a heart-wall period are generated by shifting the origin of the bounding box up at the rate of  $s$  pixels/frame, for  $\frac{T}{2} - 1$  frames and then shifting it down at the same rate for the remaining  $\frac{T}{2}$  frames.
- The created heart-wall period of  $T$  frames is repeated  $N$  times to generate the complete sequence. In this sequence, the “heart-wall” exhibits an up-down motion with period  $T$ .

### 3.3.2 RBC Data Generation

The non-periodic “RBC” sequence is generated synthetically as follows:

- First, the type of RBC particle is chosen. The particle could be circular, rectangular, Gaussian or even a textured image. The particle is then generated according to the type specified.
- The number of particles required  $P$  and the rate of motion of the particle ( $v$  pixels/frame) is chosen.
- An empty canvas of size  $W_c \times H_c$  pixels is created. Here  $W_c = W + (v \times N \times T)$  pixels and  $H_c = H$  pixels. Then the  $P$  particles are randomly placed on this canvas.
- Then starting from the origin  $(x, y) = (0, 0)$  of the canvas and a bounding box of size  $W \times H$ , the pixels in the selection are cropped to make up the frames of the RBC sequence. For every frame, the origin of the bounding box is shifted to the right by  $v$  pixels.
- In the generated sequence the “RBCs” exhibit a left to right motion.

### 3.3.3 Heartbeat Data Composition

The synthetically generated “heart-wall” and “RBC” sequences are then super-imposed frame by frame to create the final beating heart sequence. This is then passed through the different stages of the algorithm to

separate the heart-wall and RBC. The separated heart-wall and RBC sequences are then compared visually with the generated heart-wall and RBC sequences to assess the quality of separation.

## Chapter 4

# Results and Observations

Using different combinations of techniques for heart-wall and RBC separation several composite frame sequences (section 3.2) were generated. The results shown here are single frames extracted from these sequences. Figures 4.1, 4.2, 4.3 and 4.4 show the result of the algorithm on bright-field microscopy images of zebrafish heart. The original sequences in Figures 4.1 and 4.2 were captured at high speed ( $\approx 600$  fps) with a resolution of  $305 \times 253$  pixels, while those in Figures 4.3 and 4.4 were captured at reduced speed ( $\approx 43.5$  fps) with a resolution of  $176 \times 128$  pixels.

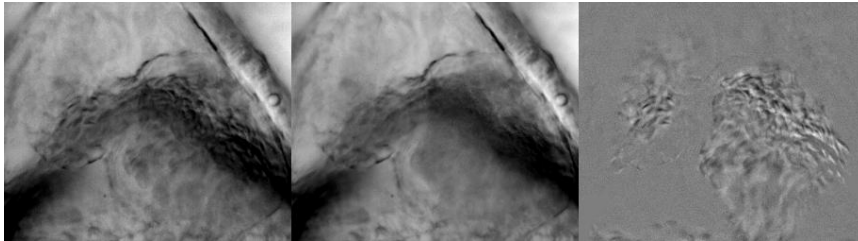


**Figure 4.1:** (L-R) Frame from original sequence, heart-wall extracted using mean filtering, RBCs extracted using subtraction method [12].

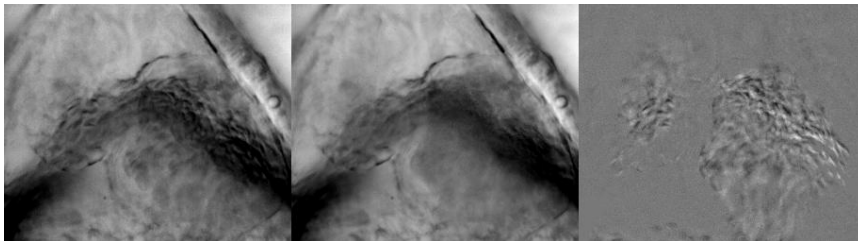


**Figure 4.2:** (L-R) Frame from original sequence, heart-wall extracted using median filtering, RBCs extracted using subtraction method [12].

The results of heart-wall extraction using mean or median filtering are quite comparable. As seen in Figures 4.1 and 4.2, the subtraction method of RBC extraction performs well but has traces of the background visible as a greyish haze around the RBCs. Figures 4.3 and 4.4 show that variance method of RBC extraction removes the background totally. However there is loss in "clarity" of RBC. Tables 4.1 and 4.2 summarize the observations.

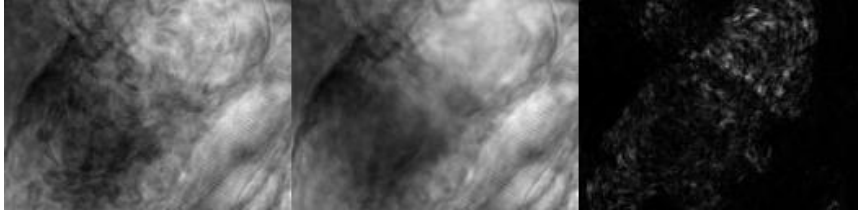


**Figure 4.3:** (L-R) Frame from original sequence, heart-wall extracted using mean filtering, RBCs extracted using variance method.

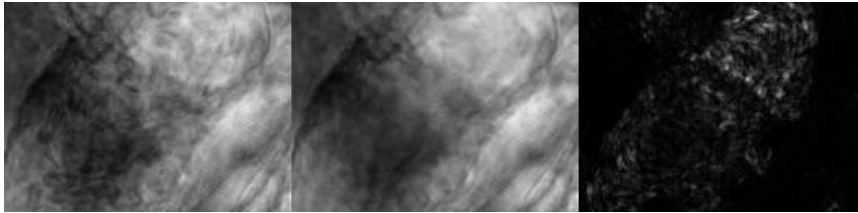


**Figure 4.4:** (L-R) Frame from original sequence, heart-wall extracted using median filtering, RBCs extracted using variance method.

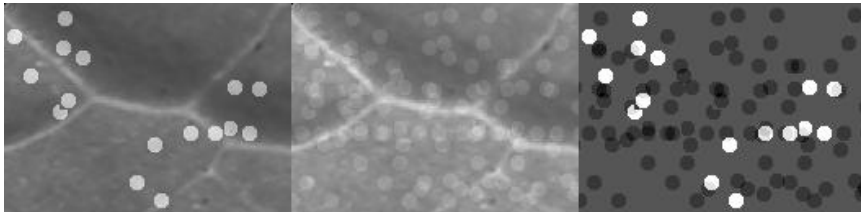
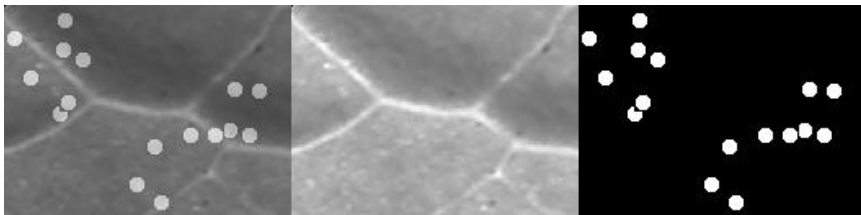
**Table 4.1:** Separation results for high frame-rate ( $\approx 600$  fps) heart-beat data

Separation techniques		For RBC	
		Subtraction method	Variance method
For Heart-wall	Mean filtering	Good separation. Traces of background seen as grayish haze in RBC data.	Good separation. No background visible in RBC data, but there is loss in clarity.
	Median filtering	Good separation. Traces of background seen as grayish haze in RBC data.	Good separation. No background visible in RBC data, but there is loss in clarity.

**Table 4.2:** Separation results for medium frame-rate ( $\approx 43.5$  fps) heart data

Separation techniques		For RBC	
		Subtraction method	Variance method
For Heart-wall	Mean filtering	Acceptable separation. Traces of background seen as grayish haze in RBC data.	Acceptable separation. No background visible in RBC data, but there is loss in clarity.
	Median filtering	Acceptable separation. Traces of background seen as grayish haze in RBC data.	Acceptable separation. No background visible in RBC data, but there is loss in clarity.

Figures 4.5, 4.6, 4.7 and 4.8 show the result of the algorithm on the synthetically generated heart sequences. As seen in the Figure 4.6, median filtering with subtraction method gives near perfect results. The extracted heart-wall and RBC sequences are identical to the original sequences (the ground-truth).

**Figure 4.5:** (L-R) Frame from synthetic heart sequence, "heart-wall" extracted using mean filtering, "RBCs" extracted using subtraction method.**Figure 4.6:** (L-R) Frame from synthetic heart sequence, "heart-wall" extracted using median filtering, "RBCs" extracted using subtraction method.

In general we see that median filtering performs better than mean filtering for heart-wall extraction. The RBC extraction for subtraction is the best with median filtering, but with the variance technique there are

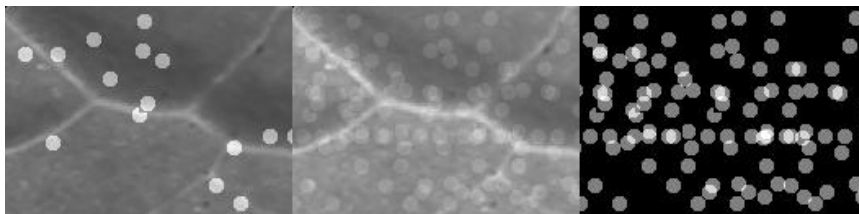


**Figure 4.7:** (L-R) Frame from synthetic heart sequence, "heart-wall" extracted using mean filtering, "RBCs" extracted using variance method.

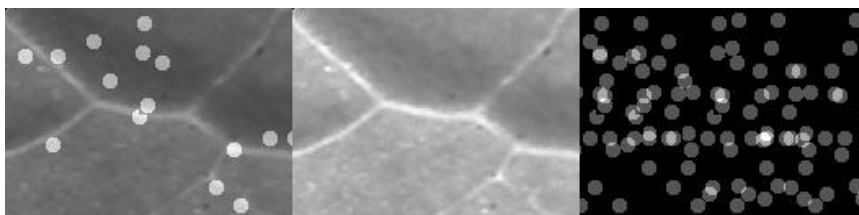


**Figure 4.8:** (L-R) Frame from synthetic heart sequence, "heart-wall" extracted using median filtering, "RBCs" extracted using variance method.

considerable contributions from RBCs present in other frames along the repeat direction as seen in Figures 4.7 and 4.8. Table 4.3 summarizes the observations.

**Table 4.3:** Separation results for synthetic heart data

Separation techniques		For RBC	
		Subtraction method	Variance method
For Heart-wall	Mean filtering	Acceptable separation. RBC traces seen in heart-wall data. "Ghosting" seen in RBC data.	Acceptable separation. RBC traces seen in heart-wall data. Black patches seen in RBC data.
	Median filtering	Excellent separation.	Bad separation. No RBC traces seen in heart-wall data. But severe "ghosting" visible in RBC data.

Figure 4.9 shows the result of the algorithm before and after flow analysis. We see in Figure 4.9b that the flow-map of the separated heart-wall or RBC is easier to analyze than the one for the original sequence.

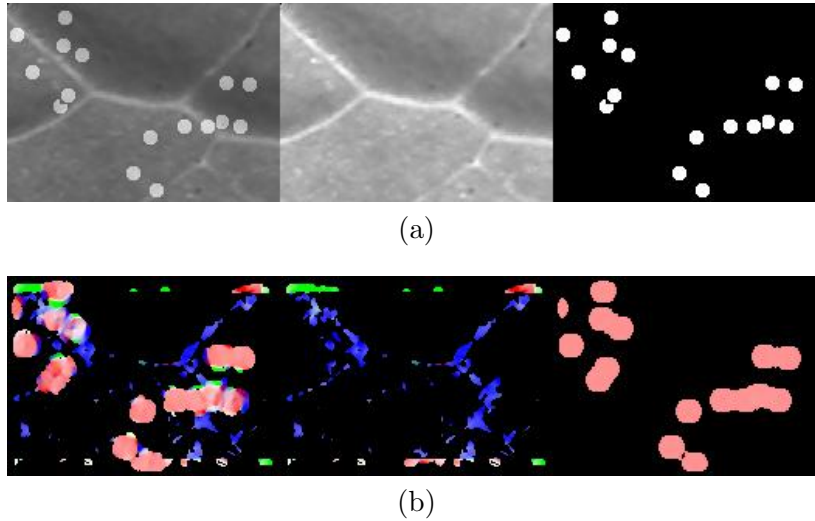


**Figure 4.9:** (L-R)Frames from synthetic heart sequence, "heart-wall" extracted using median filtering, "RBCs" extracted using subtraction method. (a) Frames as got from the algorithm. (b) Flow-maps in DC format got after flow analysis.

## Chapter 5

# Conclusion

The HW-RBC algorithm provides a technique for separation of heart-wall and RBC images from a bright-field microscopy image sequence of the beating embryonic heart. This algorithm would allow to push back the speed limitation incurred in fluorescence microscopy while overcoming the lack of specificity of brightfield microscopy in imaging unstained samples. The two image sequences obtained can be subjected to flow analysis separately, thereby enabling better characterization of blood flow and heart-wall motion in the developing zebrafish embryo.

### Acknowledgements

I want to thank Prof. Michael Liebling for giving me the opportunity to work in the Systems Bioimaging Lab, for guiding my work and for the valuable discussions that have helped me along the way. I would also want to thank Julien Vermot for sharing his zebrafish data for this work. Finally I want to thank my wife Malavika for her countless suggestions and unending support.

# Bibliography

- [1] M. Liebling, J. Vermot, A.S. Forouhar, M. Gharib, M.E. Dickinson, and S.E. Fraser. Nonuniform temporal alignment of slice sequences for four-dimensional imaging of cyclically deforming embryonic structures. In *Proceedings of the 3rd IEEE International Symposium on Biomedical Imaging: Macro to Nano (ISBI'06)*, pages 1156–1159, Arlington, VA, USA, April 6–9, 2006.
- [2] K.R. Spring and M.W. Davidson. Introduction to fluorescence microscopy. *Nikon MicroscopyU*, Oct. 2008. <http://www.microscopyu.com/>.
- [3] Maksymilian Pluta. *Advanced Light Microscopy*. Elsevier, 1988.
- [4] B. Bracegirdle S. Bradbury. *Introduction to Light Microscopy*. BIOS Scientific Publishers, 1998.
- [5] Linda G. Shapiro and George C. Stockman. *Computer Vision*, pages 279–325. Prentice-Hall, 2001.
- [6] M. Liebling, A.S. Forouhar, R. Wolleschensky, B. Zimmermann, R. Ankerhold, S.E. Fraser, M.Gharib, and M.E. Dickinson. Rapid three-dimensional imaging and analysis of the beating embryonic heart reveals functional changes during development. *Developmental Dynamics*, 235(11):2940–2948, Nov. 2006.
- [7] M. Liebling, J. Vermot, and S.E. Fraser. Double time-scale image reconstruction of the beating and developing embryonic zebrafish heart. *Biomedical Imaging: From Nano to Macro, 2008. ISBI 2008. 5th IEEE International Symposium on*, pages 855–858, May. 2008.
- [8] R.V. Hogg and A.T. Craig. *Introduction to Mathematical Statistics*, page 152. Macmillan, 1995.
- [9] R.C. Gonzalez and R.E. Woods. *Digital Image Processing*, chapter 3, pages 119–125. Prentice-Hall India, 2002.

- [10] M.D. Abramoff, W.J. Niessen, and M.A. Viergever. Objective quantification of the motion of soft tissues in the orbit. *Medical Imaging, IEEE Transactions on*, 19(10):986–995, Oct. 2000.
- [11] Laboratory for Optical and Computational Instrumentation. OME-XML format specification. *Open Microscopy Environment*, Jun. 2008.  
[openmicroscopy.org/site/documents/specifications/ome-xml-format](http://openmicroscopy.org/site/documents/specifications/ome-xml-format).
- [12] Data courtesy: Julien Vermot, Beckman Institute, California Institute of Technology. [jvermot@its.caltech.edu](mailto:jvermot@its.caltech.edu).